ACS APPLIED MATERIALS & INTERFACES

Research Article

www.acsami.org

Crack-Release Transfer Method of Wafer-Scale Grown Graphene Onto Large-Area Substrates

Jooho Lee,[†] Yongsung Kim,[†] Hyeon-Jin Shin,[†] ChangSeung Lee,[†] Dongwook Lee,[†] Sunghee Lee,[†] Chang-Yul Moon,[†] Su Chan Lee,[‡] Sun Jun Kim,[‡] Jae Hoon Ji,[‡] Hyong Seo Yoon,[‡] and Seong Chan Jun*[,‡]

[†]Samsung Advanced Institute of Technology, Yongin 446-577, South Korea

[‡]School of Mechanical Engineering, Yonsei University, Seoul 120-749, South Korea

ABSTRACT: We developed a crack-release graphene transfer technique for opening up possibilities for the fabrication of graphene-based devices. Graphene film grown on metal catalysts/SiO_2/Si wafer should be scathelessly peeled for sequent transferring to a target substrate. However, when the graphene is grown on the metal catalyst on a silicon substrate, there is a large tensile stress resulting from the difference of the coefficient of thermal expansion in the catalyst and silicon. The conventional methods of detaching graphene from metal catalysts were found to induce considerable mechanical damage on graphene films during separation processes including metal wet etching. Here we report a new technique wherein bubbles generated by electrolysis reaction separate thin metal catalysts from the SiO_2/Si wafer. The dry attachment of graphene to the target wafer was processed utilizing a wafer to wafer bonding technique in a vacuum. We measured the microscopic image, Raman spectra, and electrical properties of the transferred graphene. The optical and electrical properties of the graphene transferred by the bubbles/dry method are better than those of the graphene obtained by mechanical/wet transfer.

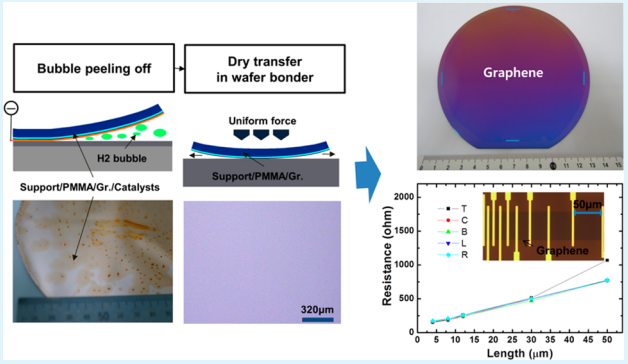

KEYWORDS: *graphene, crack-release, electrolysis, bubble, dry attachment*

1. INTRODUCTION

Graphene is a promising material that has a hexagonal carbon structure, and it has the atomic thickness of several angstroms.[1−3] Graphene shows the most brilliant electrical properties compared to the other materials, and its conductivity is 100 times higher than crystalline silicon.[4−8] Its breakdown strength is much higher than that of copper, so it is more and more focused on as the basic material for electronic circuit devices.[9] When we consider the recent industry issues for electronic devices such as graphene field effect transistors (FETs)[10,11] and graphene barristors,[12] the main problem for graphene is how to obtain a monolayer graphene film on large-area wafers. The chemical vapor deposition (CVD) growth of graphene on metal foils and transfer to a rigid substrate have been known as the most famous method to obtain better monolayer graphene quality.[13−17] However, the monolayer graphene was hard to obtain uniformly on a flexible and thick metal foil due to the high surface roughness of the foil sheet as well as undesired defects such as long-range wrinkle and tearing occuring during transfer to rigid substrates.[18] Even though the surface roughness of graphene originating from metal catalyst morphology could be minimized using a thin metal catalyst on rigid SiO_2/Si substrate,[19−21] transfer problems still remain. Direct growth of graphene on SiO_2 and/or Si substrate has been demonstrated to remove defect formation during the transfer process.[22−25] Although high-quality monolayer graphene is directly grown on substrates, the growth temperature and conditions are too harsh to apply to real device processes. Direct growth at low temperatures using mild conditions and improvement of the transfer process without defects are still needed for semiconductor manufacturing processes.

To circumvent macroscopic defect generation during graphene transfer, delamination methods were developed to transfer graphene grown on metal onto other substrates.[26−29] However, the electrochemical delamination of graphene from a flexible metal foil could not guarantee the perfect transfer on a large-area substrate without macroscopic defects since handling PMMA and graphene without a supporting layer produces wrinkles and cuts in graphene.

Besides, it is almost impossible to adopt water-free dry transfer owing to the lack of a handling support which could assist during conventional bonding or the taping process without water. Here, we report a stress-released transfer process of graphene for control of defect generation, overcoming the disadvantages of conventional wafer-scale synthesis and transfer of graphene films.

Received: April 28, 2014
Accepted: June 26, 2014
Published: June 26, 2014

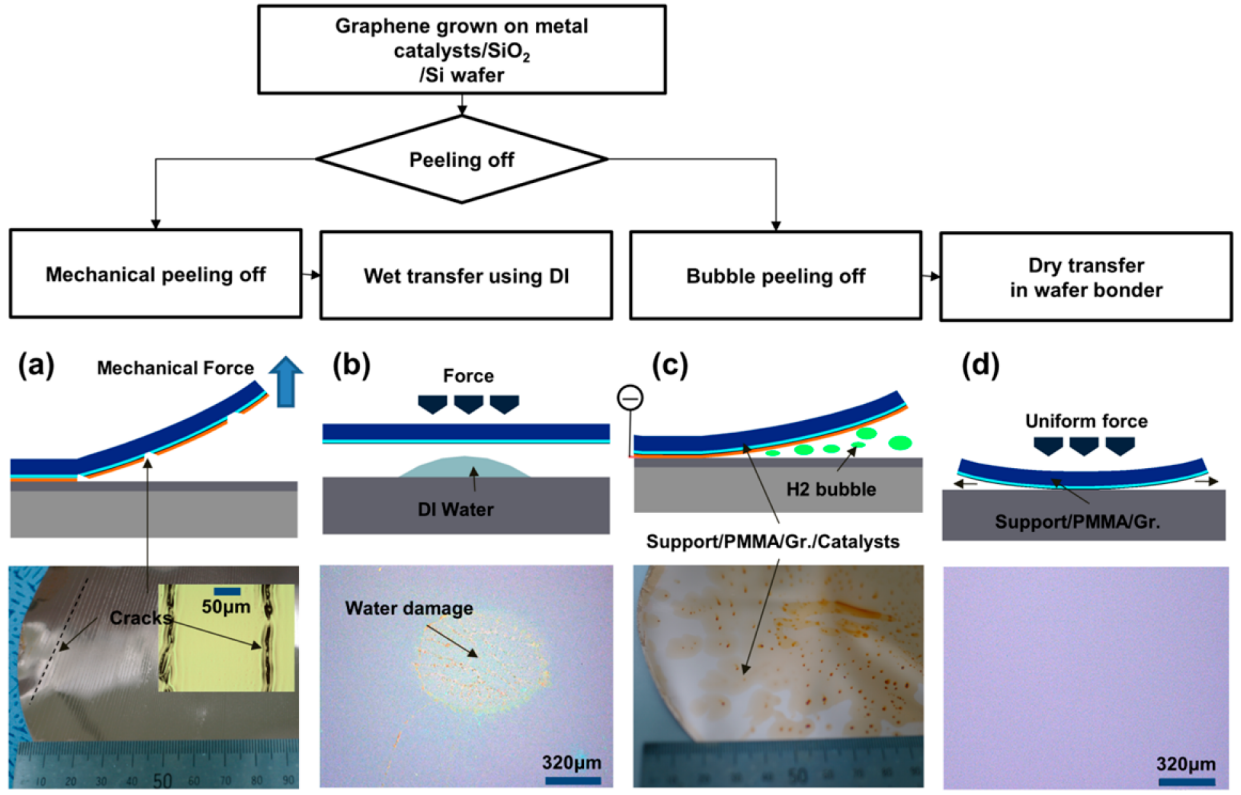

Figure 1. Flowchart of the transfer process. (a) Schematic illustration of mechanical peeling. Photograph and (inset) optical microscopy image of a separated catalyst/graphene/PMMA/support stack showing the presence of cracks during the mechanical peeling process. (b) Schematic illustration of wet transfer using water. Optical microscope image of wet transferred graphene with undesired defects. (c) Schematic illustration of the bubbling method. Optical image of a catalyst/graphene/PMMA/support stack separated from a large wafer by bubbling method showing excellent continuity with very few cracks. (d) Schematic illustration of the dry transfer process utilizing a wafer bonder. Optical microscope image of graphene transferred on SiO_2/Si wafers showing the uniform color contrast.

2. EXPERIMENTAL SECTION

2.1. Synthesis of Graphene by the ICP-CVD Process. Graphene was synthesized by inductively coupled plasma chemical vapor deposition (ICP-CVD) where we adopted low-temperature-plasma-assisted growth.[30] The substrate for graphene growth was prepared by electron beam evaporation of Ni 200 Å/Cu 3000 Å on a 6 in. SiO_2/Si (5000 Å thick thermally grown SiO_2 layer) substrate. We were able to grow monolayer graphene with a Ni concentration less than 10 at %. The substrate was loaded into ICP-CVD, and it was evacuated to $\sim 10^{-7}$ Torr using a turbo-molecular pump. The substrate temperature was increased from room temperature to the growth temperature at a rate of 50 °C/min. The metal catalyst film was treated with hydrogen plasma (100 W plasma power) for 1 min with the wafer heated to 750 °C at 50 mTorr in order to clean the oxide on the catalyst surface. The mixture of C_2H_2 and Ar (C_2H_2:Ar = 1:40) was introduced into the chamber and stabilized. Graphene film was then synthesized in the plasma (100 W plasma power, 50 mTorr, 3 min) at the same temperature. After growth was completed, the substrate was cooled down to room temperature over 3 h at a pressure of $\sim 10^{-7}$ Torr.

2.2. Graphene Transfer from Metal Catalysts to the SiO_2/Si Wafer. For graphene transfer, poly(methyl methacrylate) (PMMA) was spin-coated on the graphene at 4000 rpm for 40 s and cured at 120 °C for 3 min. An ultraviolet (UV) release tape (Hugle Protection Tape HUP-1252S) as a polymer support was attached onto it. Figure 1 schematically shows the sequential stress-release process for transferring graphene onto the 6 in. SiO_2/Si wafer. Figure 1a illustrates mechanical peel-off. The image of a separated catalyst/graphene/PMMA/support stack displays cracks generated while separating graphene from a large-area substrate. When graphene was peeled off using mechanical force, cracks occurred on the wafer. Figure 1b shows a conventional wet transfer process using deionized (DI) water. Conventionally, DI water should be spread on the wafer surface to promote good adhesion between the graphene and oxide layers of wafers in order to transfer graphene onto another wafer. However, defects such as water contamination and air traps deteriorate graphene. The damaged graphene resulting from the water is shown in Figure 1b. Figure 1c schematically illustrates the bubbling peel-off method. The catalyst/graphene/PMMA/support was separated from a substrate by enhancing bubbles between catalyst and SiO_2 layer as shown in Figure 1c. The metal catalyst/graphene/PMMA/support was used as the cathode with an aqueous solution of $K_2S_2O_8$ (0.4 mM).[31] The metal catalyst electrode was polarized at −5 V, and hydrogen bubbles were generated at the Cu/SiO_2 interfaces. During the bubbling process, a chemical etching and an electrochemical deposition were processed on the surface of the copper catalyst, simultaneously.

$$2H_2O(l) + 2e \rightarrow H_2(g) + 2OH^- \quad (1)$$

$$Cu + S_2O_8^{2-}(aq) \rightarrow Cu^{2+} + 2SO_4^{2-}(aq) \quad (2)$$

$$3Cu^{2+}(aq) + 4OH^{-}(aq) + 2e - \rightarrow Cu_2O(s) + CuO(s) + 2H_2O(l) \quad (3)$$

After the catalyst/graphene/PMMA/support was separated from a substrate, the metal catalyst was removed in the diluted $FeCl_3$ solution.

The remaining graphene/PMMA/UV tape was dried at a room temperature. Figure 1d is the schematic of the dry transfer step. The OH-terminated SiO_2 surface of a target substrate was prepared by a standard cleaning process, which was done in the standard clean bath (NH_4OH:H_2O_2:DI = 1:1:5) and in piranha bath (H_2SO_4:H_2O_2 = 4:1) followed by a standard cleaning procedure, rinsing in DI water, and drying in a spin dryer. The attachment of graphene onto the target wafer was processed utilizing a silicon wafer bonder (EVG TM 501) at room temperature. The graphene/PMMA/support placed between an OH-terminated, 6 in. SiO_2 wafer and a ceramic plate was pressed under the pressure of 200 N/mm^2 from the middle to the edge in a vacuum chamber (~3 mTorr). After the pressing process, the tape was then separated from graphene/PMMA in hot methanol and the PMMA was also removed with acetone. The graphene wafer was annealed in a 250 °C vacuum furnace for 3 h to burn out the residual PMMA on the transferred graphene. Figure 1d shows a microscopic image of graphene transferred by a water-free dry transfer method with a vacuum bonder. The uniform color contrast of the optical micrograph in Figure 1d indicates that the film has a uniform thickness. Moreover, the process time to remove adhesive water could be dramatically reduced from 12 to 1 h by excluding the DI water in the transferred graphene. This process can be applied to a SiO_2/Si substrate as well as a glass substrate. We could minimize contamination, damage, and cracks on a dry-transferred graphene separated from a large wafer by the bubbling method, which was different from a conventional wetting transfer method using bubbles.

2.3. Material Characterization. Structural and topological properties of the sample were characterized with X-ray diffraction (XRD, X'Pert Pro MPD, Cu Kα, 40 kV, 40 mA), field-emission scanning electron microscope (FESEM, S4700, Hitachi), and a thin film stress measurement system (Tencor FLX-232). The morphology of graphene films was investigated by atomic force microscope (AFM, Seiko Instruments Inc.). The crystallinity of the graphene layers was analyzed by performing Raman spectroscopy after transferring the films to a SiO_2/Si substrate. The Raman spectra and mapping images of graphene films were created using Raman spectroscopy (Renishaw, RM-1000Invia) with an excitation energy of 2.41 eV (514 nm, Ar^+ ion laser). The sheet resistance and contact resistance were calculated by transfer length method (Keithley 4200).

3. RESULTS AND DISCUSSION

Figure 2a shows the crystallographic characteristics of metal catalysts before/after ICP-CVD growth of graphene. The (111) peak of Cu becomes more dominant, while the (311) peak of Cu becomes negligible after graphene growth. Since grains of Cu catalyst are reoriented to be in a low energy facet during the growth, residual stress remains after the growth process. The SEM images are depicted in Figure 2b, comparing the surface before and after graphene growth on metal catalysts. The grain size of the metal catalyst increased after graphene growth. Figure 2d indicates deflection of the substrate, which was

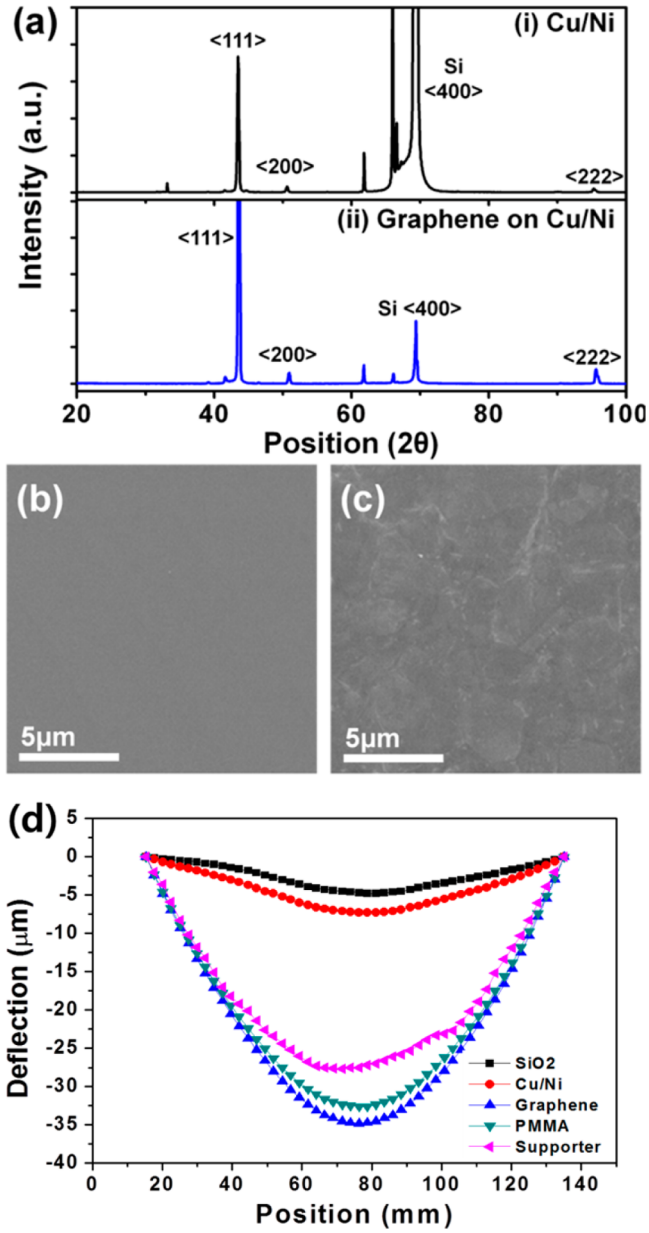

Figure 2. Characteristics of graphene. (a) XRD patterns of the wafers: before graphene growth (upper), after graphene growth (lower). (b) SEM images of Cu/Ni alloy before graphene growth. (c) SEM images of graphene grown on Cu/Ni alloy. (d) Curves measured with the thin film stress measurement system by the process steps, respectively.

measured step by step after each process. SiO_2 and Cu underwent minor deflection (~7 um), while graphene, PMMA, and the support suffered severe deflection. Residual stresses in each layer were calculated, and values of the stresses are presented in Table 1. The average stress (σ_f) of each film was also calculated using the Stoney equation. The residual stress of the metal catalyst after graphene growth was 733.7 MPa (tensile), which was high enough to generate mechanical cracking on a graphene layer during separation of graphene from a large-area substrate.

Figure 3a shows a photograph of graphene transferred onto a 6 in. wafer by the proposed method. Graphene is within the guidelines at the sides. The atomic force microscope (AFM) image in Figure 3c displays uniformly transferred graphene with low roughness. The quality of graphene was characterized by

Table 1. Wafer Bow and Residual Stresses Corresponding to Layers

		thickness	temp (°C)	bow (μm)	stress (MPa)
SiO_2	wet oxidation	5000 Å ± 5%	1000	−4.8	
CuNi	evaporation	3200 Å ± 10%	RT	−7.3	62.4
CuNi/ Graphene	ICP-CVD	~3200 Å	750	−34.8	733.7
PMMA	spin coat/ bake	2200 Å ± 5%	120	−32.6	−77.2
supporter	tape mounter	95 ± 13 μm	RT	−27.7	−4.1

Raman spectroscopy. Figure 3b illustrates a sharp 2D peak and high ratio of 2D/G, which demonstrate that graphene is monolayer.[32,33] The micro-Raman maps of the G peak (Figure 3d) and 2D peak (Figure 3e) over about a 20 μm × 20 μm area also show that graphene was more uniformly transferred, minimizing the defects or cracks. Optical microscope images in Figure 3f and g compare morphologies of the graphene films transferred onto SiO_2/Si wafers by the bubble/dry and mechanical/wet processes, respectively. The uniform color contrast of Figure 3f indicates that the film has the excellent thickness uniformity over the wafer. The above experimental results ascertain that we could guarantee the transferred graphene with a much lower density of large cracks or tears using the bubble/dry transfer process.

Transfer length method (TLM) structures were fabricated to characterize electrical properties of graphene transferred by the proposed method,[34,35] as shown in Figure 4a. The graphene was patterned by oxygen plasma to construct Au/Cr/Al electrodes.[36] Resistances were measured according to the length of graphene at five different positions for top (T), center (C), bottom (B), left (L), and right (R) on wafer. The contact resistance (Rc) and sheet resistance (Rs) were extracted from TLM patterns. TLM patterns in Figure 4a had a width of W = 50 μm and resistor lengths of L1 = 4 μm, L2 = 8 μm, L3 = 12 μm, L4 = 30 μm, and L5 = 50 μm, respectively. Figure 4b and c compare resistances of graphene transferred by the proposed method with those of mechanically transferred graphene. The slope of the line is the sheet resistance of the graphene, and the

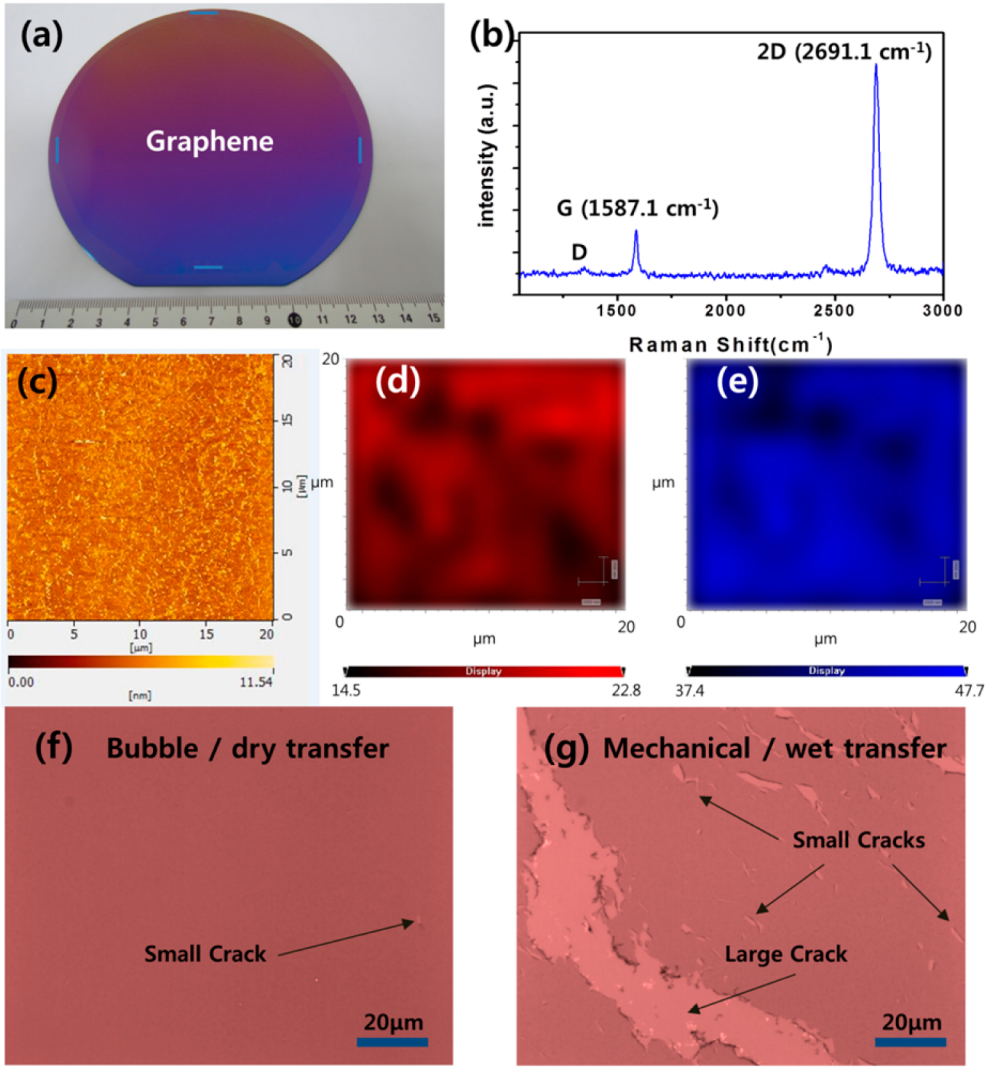

Figure 3. (a) Photograph of graphene transferred to 6 in. SiO_2/Si substrate using the proposed process. (b) Raman spectrum of graphene transferred using the proposed process. (c) AFM image of transfered graphene. (d) G-band and (e) 2D-band energies on the area of 20 μm × 20 μm. Comparisons of the transferred graphene quality obtained using the different transfer methods. (f) Optical microscope image of the area in part a. (g) Optical microscope image of graphene transferred using mechanical peeling and wet transfer process.

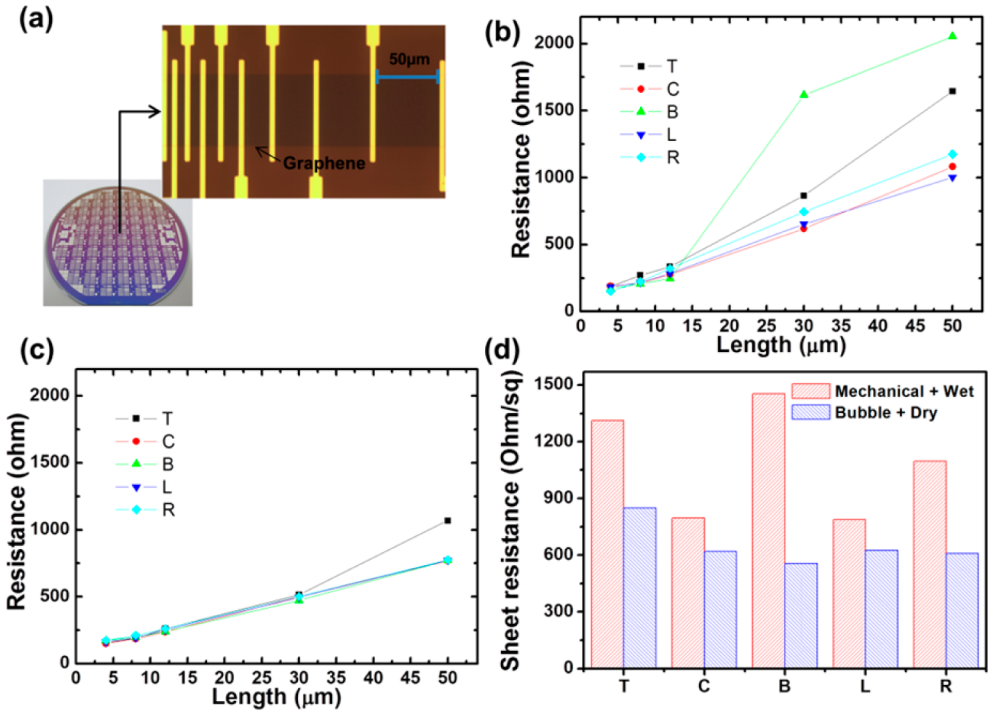

Figure 4. Electrical properties of graphene. (a) Optical microscope image of a TLM structure on the graphene fabricated on a 6 in. SiO_2/Si substrate. (b) Resistance distribution of the transferred graphene obtained using the mechanical peeling and wet transfer process. (c) Resistance distribution of the transferred graphene obtained using the bubble peeling and dry transfer. (d) Comparisons of sheet resistance histogram derived using TLM.

y-axis offset represents the value of 2Rc. As the patterned length increased, the values of the measured resistance also increased. However, there was a difference of the uniformity of the measured resistance in accordance with the transfer method. The results from TLM shown in Figure 4b show relatively large fluctuations due to the formation of defects of the graphene, while Figure 4c shows a linear relationship between Rc and the measured resistances. The contact resistances were obtained by a linear fit in Figure 4b and c. The values range from 41.1 to 54.4 Ω.

Figure 4d presents histograms of the sheet resistance of the graphene film transferred onto a 6 in. SiO_2/Si wafer. The sheet resistance of graphene transferred by bubble/dry process shows the uniformity distribution around 650 Ω/square, which is comparable to the value obtained from the mechanical/wet transferred wafer level process. The average sheet resistance of graphene transferred by bubble/dry process was 651.8 Ω/square, and the standard deviation was 114.0 Ω/square; meanwhile the mechanical/wet process transferred wafer showed 1089.2 Ω/square and a standard deviation of 299.3 Ω/square, respectively. The density of defects such as cracks, contamination, and tears could be minimized utilizing the separation with bubbles and dry bonding scheme, leading to stable sheet resistance of graphene. The bubble/dry transferred graphene films show uniform electrical properties across a large area, suggesting that the transferred graphene could be applied to graphene electronic devices on large-scale substrates. Consequently, we suggest this as an effective method of transferring graphene films onto a substrate as large as 6 in.

4. CONCLUSION

In this work, we suggest an effective method of transferring graphene films onto a substrate as large as 6 in. The ICP-CVD process in synthesizing the graphene to minimize deformation of the substrate enabled graphene growth on a large substrate. The bubbles generated by electrolysis reaction separated the thin metal catalyst from the wafer to minimize mechanical cracks. In addition, the dry transfer process using a wafer bonding technique in a vacuum could decrease air trap defects and process time. The transferred graphene was uniform across an entire wafer. Moreover, macroscopic defects such as cuts, tears, and wrinkles were dramatically decreased. The proposed method is expected to be applied to fabrication of wafer-scale graphene-based electronic devices.

AUTHOR INFORMATION

Corresponding Author

*Tel.: +82-2-2123-5817. Fax: +82-2-312-2159. E-mail: scj@yonsei.ac.kr.

Notes

The authors declare no competing financial interest.

ACKNOWLEDGMENTS

This work was partially supported by the Pioneer Research Center Program (2010-0019313) and the Priority Research Centers Program (2009-0093823) through the National Research Foundation (NRF) of Korea funded by the Ministry of Science, ICT & Future Planning.

REFERENCES

(1) Novoselov, K. S.; Geim, A. K.; Morozov, S.; Jiang, D.; Zhang, Y.; Dubonos, S.; Grigorieva, I.; Firsov, A. Electric Field Effect in Atomically Thin Carbon Films. *Science* **2004**, *306* (5696), 666−669.

(2) Zhang, Y.; Tan, Y.-W.; Stormer, H. L.; Kim, P. Experimental Observation of the Quantum Hall Effect and Berry's Phase in Graphene. *Nature* **2005**, *438* (7065), 201−204.

(3) Geim, A. K. Graphene: Status and Prospects. *Science* **2009**, *324* (5934), 1530−1534.

(4) Geim, A. K.; Novoselov, K. S. The Rise of Graphene. *Nat. Mater.* **2007**, *6* (3), 183−191.
(5) Blake, P.; Brimicombe, P. D.; Nair, R. R.; Booth, T. J.; Jiang, D.; Schedin, F.; Ponomarenko, L. A.; Morozov, S. V.; Gleeson, H. F.; Hill, E. W.; Geim, A. K.; Novoselov, K. S. Graphene-Based Liquid Crystal Device. *Nano Lett.* **2008**, *8* (6), 1704−1708.
(6) Wang, X.; Zhi, L.; Müllen, K. Transparent, Conductive Graphene Electrodes for Dye-Sensitized Solar Cells. *Nano Lett.* **2008**, *8* (1), 323−327.
(7) Kim, K. S.; Zhao, Y.; Jang, H.; Lee, S. Y.; Kim, J. M.; Kim, K. S.; Ahn, J.-H.; Kim, P.; Choi, J.-Y.; Hong, B. H. Large-Scale Pattern Growth of Graphene Films for Stretchable Transparent Electrodes. *Nature* **2009**, *457* (7230), 706−710.
(8) Kim, W. K.; Jung, Y. M.; Cho, J. H.; Kang, J. Y.; Oh, J. Y.; Kang, H.; Lee, H.-J.; Kim, J. H.; Lee, S.; Shin, H. Radio-Frequency Characteristics of Graphene Oxide. *Appl. Phys. Lett.* **2010**, *97* (19), 193103.
(9) Sharma, M.; Ghosh, S. Electron Transport and Goos−Hänchen Shift in Graphene with Electric and Magnetic Barriers: Optical Analogy and Band Structure. *J. Phys.: Condens. Matter* **2011**, *23* (5), 055501.
(10) Lin, Y.-M.; Dimitrakopoulos, C.; Jenkins, K. A.; Farmer, D. B.; Chiu, H.-Y.; Grill, A.; Avouris, P. 100-GHz Transistors from Wafer-Scale Epitaxial Graphene. *Science* **2010**, *327* (5966), 662−662.
(11) Huang, Y.; Dong, X.; Shi, Y.; Li, C. M.; Li, L.-J.; Chen, P. Nanoelectronic Biosensors Based on CVD grown Graphene. *Nanoscale* **2010**, *2* (8), 1485−1488.
(12) Yang, H.; Heo, J.; Park, S.; Song, H. J.; Seo, D. H.; Byun, K.-E.; Kim, P.; Yoo, I.; Chung, H.-J.; Kim, K. Graphene Barristor, a Triode Device with a Gate-Controlled Schottky Barrier. *Science* **2012**, *336* (6085), 1140−1143.
(13) Reina, A.; Jia, X.; Ho, J.; Nezich, D.; Son, H.; Bulovic, V.; Dresselhaus, M. S.; Kong, J. Large Area, Few-layer Graphene Films on Arbitrary Substrates by Chemical Vapor Deposition. *Nano Lett.* **2008**, *9* (1), 30−35.
(14) Li, X.; Cai, W.; An, J.; Kim, S.; Nah, J.; Yang, D.; Piner, R.; Velamakanni, A.; Jung, I.; Tutuc, E.; Banerjee, S. K.; Colombo, L.; Ruoff, R. S. Large-Area Synthesis of High-Quality and Uniform Graphene Films on Copper Foils. *Science* **2009**, *324* (5932), 1312−1314.
(15) Bae, S.; Kim, H.; Lee, Y.; Xu, X.; Park, J.-S.; Zheng, Y.; Balakrishnan, J.; Lei, T.; Kim, H. R.; Song, Y. I.; Kim, Y.-J.; Kim, K. S.; Ozyilmaz, B.; Ahn, J.-H.; Hong, B. H.; Iijima, S. Roll-to-Roll Production of 30-in. Graphene Films for Transparent Electrodes. *Nat. Nanotechnol.* **2010**, *5* (8), 574−578.
(16) Verma, V. P.; Das, S.; Lahiri, I.; Choi, W. Large-area Graphene on Polymer Film for Flexible and Transparent Anode in Field Emission Device. *Appl. Phys. Lett.* **2010**, *96* (20), 203108.
(17) Kang, J.; Hwang, S.; Kim, J. H.; Kim, M. H.; Ryu, J.; Seo, S. J.; Hong, B. H.; Kim, M. K.; Choi, J.-B. Efficient Transfer of Large-Area Graphene Films onto Rigid Substrates by Hot Pressing. *ACS Nano* **2012**, *6* (6), 5360−5365.
(18) Suk, J. W.; Kitt, A.; Magnuson, C. W.; Hao, Y.; Ahmed, S.; An, J.; Swan, A. K.; Goldberg, B. B.; Ruoff, R. S. Transfer of CVD-Grown Monolayer Graphene onto Arbitrary Substrates. *ACS Nano* **2011**, *5* (9), 6916−6924.
(19) Levendorf, M. P.; Ruiz-Vargas, C. S.; Garg, S.; Park, J. Transfer-Free Batch Fabrication of Single Layer Graphene Transistors. *Nano Lett.* **2009**, *9* (12), 4479−4483.
(20) Lee, Y.-H.; Lee, J.-H. Scalable Growth of Free-standing Graphene Wafers with Copper (Cu) Catalyst on SiO_2/Si Substrate: Thermal Conductivity of the Wafers. *Appl. Phys. Lett.* **2010**, *96* (8), 083101.
(21) Lee, Y.; Bae, S.; Jang, H.; Jang, S.; Zhu, S.-E.; Sim, S. H.; Song, Y. I.; Hong, B. H.; Ahn, J.-H. Wafer-Scale Synthesis and Transfer of Graphene Films. *Nano Lett.* **2010**, *10* (2), 490−493.
(22) Ismach, A.; Druzgalski, C.; Penwell, S.; Schwartzberg, A.; Zheng, M.; Javey, A.; Bokor, J.; Zhang, Y. Direct Chemical Vapor Deposition of Graphene on Dielectric Surfaces. *Nano Lett.* **2010**, *10* (5), 1542−1548.
(23) Su, C.-Y.; Lu, A.-Y.; Wu, C.-Y.; Li, Y.-T.; Liu, K.-K.; Zhang, W.; Lin, S.-Y.; Juang, Z.-Y.; Zhong, Y.-L.; Chen, F.-R.; Li, L.-J. Direct Formation of Wafer Scale Graphene Thin Layers on Insulating Substrates by Chemical Vapor Deposition. *Nano Lett.* **2011**, *11*, 3612−3616.
(24) Pan, G.; Li, B.; Heath, M.; Horsell, D.; Wears, M. L.; Taan, L. A.; Awan, S. Transfer-Free Growth of Graphene on SiO_2 Insulatior Substrate from Sputtered Carbon and Nickel films. *Carbon* **2013**, *65*, 349−358.
(25) Kim, H.; Song, I.; Park, C.; Son, M.; Hong, M.; Kim, Y.; Kim, J. S.; Shin, H.-J.; Baik, J.; Choi, H. C. Copper-vapor-assisted Chemical Vapor Deposition for High-quality and Metal-free Single-layer Graphene on Amorphous SiO_2 substrate. *ACS Nano* **2013**, *7* (8), 6575−6582.
(26) Wang, Y.; Zheng, Y.; Xu, X.; Dubuisson, E.; Bao, Q.; Lu, J.; Loh, K. P. Electrochemical Delamination of CVD-Grown Graphene Film: Toward the Recyclable Use of Copper Catalyst. *ACS Nano* **2011**, *5* (12), 9927−9933.
(27) Gao, L.; Ren, W.; Xu, H.; Jin, L.; Wang, Z.; Ma, T.; Ma, L.-P.; Zhang, Z.; Fu, Q.; Peng, L.-M. Repeated Growth and Bubbling Transfer of Graphene with Millimetre-Size Single-Crystal Grains using Platinum. *Nat. Commun.* **2012**, *3*, 699.
(28) de la Rosa, C. J. L.; Sun, J.; Lindvall, N.; Cole, M. T.; Nam, Y.; Löffler, M.; Olsson, E.; Teo, K. B.; Yurgens, A. Frame Assisted H_2O Electrolysis Induced H_2 Bubbling Transfer of Large Area Graphene Grown by Chemical Vapor Deposition on Cu. *Appl. Phys. Lett.* **2013**, *102* (2), 022101.
(29) Gao, L.; Ni, G.-X.; Liu, Y.; Liu, B.; Neto, A. C.; Loh, K. P. Face-to-Face Transfer of Wafer-Scale Graphene Films. *Nature* **2014**, *505*, 190−194.
(30) Woo, Y. S.; Seo, D. H.; Yeon, D.-H.; Heo, J.; Chung, H.-J.; Benayad, A.; Chung, J.-G.; Han, H.; Lee, H.-S.; Seo, S.; Choi, J.-Y. Low Temperature Growth of Complete Monolayer Graphene Films on Ni-Doped Copper and Gold Catalysts by a Self-Limiting Surface Reaction. *Carbon* **2013**, *64*, 315−323.
(31) De Jongh, P.; Vanmaekelbergh, D.; Kelly, J. Cu_2O: Electrodeposition and Characterization. *Chem. Mater.* **1999**, *11* (12), 3512−3517.
(32) Roddaro, S.; Pingue, P.; Piazza, V.; Pellegrini, V.; Beltram, F. The Optical Visibility of Graphene: Interference Colors of Ultrathin Graphite on SiO_2. *Nano Lett.* **2007**, *7* (9), 2707−2710.
(33) Blake, P.; Hill, E. W.; Castro Neto, A. H.; Novoselov, K. S.; Jiang, D.; Yang, R.; Booth, T. J.; Geim, A. K. Making Graphene Visible. *Appl. Phys. Lett.* **2007**, *91* (6), 063124−063124−3.
(34) Moon, J. S.; Antcliffe, M.; Seo, H. C.; Curtis, D.; Lin, S.; Schmitz, A.; Milosavljevic, I.; Kiselev, A. A.; Ross, R. S.; Gaskill, D. K.; Campbell, P. M.; Fitch, R. C.; Lee, K.-M.; Asbeck, P. Ultra-Low Resistance Ωic Contacts in Graphene Field Effect Transistors. *Appl. Phys. Lett.* **2012**, *100* (20), 203512.
(35) Schroder, D. K. *Semiconductor material and device characterization*; John Wiley & Sons, Inc.: Hoboken, NJ, 2006; Chapter 3.
(36) Lee, J.; Kim, Y.; Shin, H.-J.; Lee, C.; Lee, D.; Moon, C.-Y.; Lim, J.; Jun, S. C. Clean Transfer of Graphene and its Effect on Contact Resistance. *Appl. Phys. Lett.* **2013**, *103* (10), 103104.